

Time arrival of slab avalanche masses

D. M. McClung

Department of Geography, University of British Columbia, Vancouver, British Columbia, Canada

Received 7 November 2002; revised 18 April 2003; accepted 30 April 2003; published 9 October 2003.

[1] One of three criteria to demonstrate self-organized criticality (SOC) for a critical phenomenon is that time arrival of events displays a frequency dependence which is inversely proportional to frequency (f) to some power. That is, for SOC, the power spectrum in the frequency (f) domain is supposed to fall off as $1/f^\beta$, where β is typically a number between 1 and 2. Avalanche phenomena have been used as prototypes for illustrating SOC, and therefore it is of interest as to whether snow avalanches follow the criterion. In this paper, time series analyses of mass arrivals from 20 years of records constituting $\sim 10,000$ avalanches are presented for Bear Pass and Kootenay Pass, British Columbia. The results suggest that the autocorrelation functions and partial autocorrelation functions of the series fall off in an exponential manner so that the implied power spectra in the frequency domain, given by the Fourier transforms of the autocorrelation functions, decay with frequency in a manner which is not strictly consistent with SOC. In common with SOC, the power spectra are suggested to have most content in the low-frequency events and the spectra do not constitute white noise. However, given the limitations on the data sampling and recording, it cannot be definitively stated that the power spectra fall off with $1/f^\beta$ as required for SOC. *INDEX TERMS*: 1827 Hydrology: Glaciology (1863); 3250 Mathematical Geophysics: Fractals and multifractals; 5104 Physical Properties of Rocks: Fracture and flow; *KEYWORDS*: snow avalanches, time series, self-organized criticality

Citation: McClung, D. M., Time arrival of slab avalanche masses, *J. Geophys. Res.*, 108(B10), 2466, doi:10.1029/2002JB002299, 2003.

1. Introduction

[2] Sandpile avalanches were used as a prototype by modeling to illustrate the concept of self-organized criticality by *Bak et al.* [1987, 1988]. Later [e.g., *Bak*, 1996; *Jensen*, 1998] it was found that actual sandpile avalanches do not follow SOC and further [*McClung*, 2003a] it has been suggested that snow avalanches also do not follow SOC. Snow avalanches consist of two types: (1) loose snow avalanches releasing in cohesionless material at the top of the snowpack and (2) slab avalanches which release by propagation of shear fractures originating in a thin weak layer at depth in the snowpack to release a cohesive block of snow. *McClung* [2003a] showed that slab avalanches do not completely conform to the original description of SOC. It is unlikely that loose snow avalanches follow all the criteria for SOC since they are physically similar to sandpile avalanches. Field observations on loose snow avalanches show they are nearly all of similar size for the same physical conditions on the surface of the snowpack which suggests (but does not prove) that they are subject to inertial effects which limit the range of possible sizes similar to sandpile avalanches. For sandpile avalanches inertial effects prevent a spectrum of sizes being formed which cuts off SOC [*Jensen*, 1998]. The argument for noncompliance with

SOC for these natural phenomena (sandpiles, loose and slab avalanches) has been based on suggestions that individual releases involve a length scale which governs size, and inertial effects which prevent avalanches from forming in a large number of different sizes for a given applied perturbation and physical system. The result seems to be that some of the principles for SOC are followed by natural events but, strictly speaking, not all aspects are followed. In this paper, an entirely different aspect implied for SOC is analyzed, namely, the time arrival aspect.

[3] Complete demonstration of self-organized criticality as defined by *Bak et al.* [1987, 1988] consists of three parts:

[4] 1. For SOC, the phenomenon must exhibit critical behavior. *McClung* [2003a] showed that critical behavior as defined by *Bak et al.* [1987, 1988] is not satisfied for slab avalanches. Slab avalanches have a length scale associated with their release: the depth to the weak layer they fail on which limits their size and prevents access to a large number of metastable states and different avalanche sizes [e.g., *Jensen*, 1998] so that criticality, as envisioned by *Bak et al.* is not possible over short timescales.

[5] 2. Scale-invariant (or fractal) behavior is implied in relation to event sizes for systems following SOC. For example, a log-log plot of exceedance probability versus size should be linear (implying scale-invariant or fractal behavior) over several orders of magnitude of the fundamental dimension of size chosen to represent the phenomenon. This aspect is called spatial self-similarity by *Bak et al.*

[1988]. *McClung* [2003a] considered spatial self-similarity for slab avalanches with linkage to the fundamental release mechanism of shear fracture propagation in the weak layer found beneath slabs which release. *Bažant et al.* [2003] and *McClung* [2003a] showed that there is a fundamental length scale associated with dry slab initiation: the slab thickness, *D*. *McClung* [2003a] showed that slab avalanche sizes are not scale-invariant with *D* over any significant range of sizes.

[6] 3. For SOC, arrival of events, when looked at in the frequency domain, have a power spectrum which falls off with a negative power of frequency called $1/f$ noise or “flicker noise.” Mathematically, it is implied that the power spectrum of arrivals in the frequency domain falls off with an algebraic power law as $\sim 1/f^\beta$ where β is typically fractal between 1 and 2 [*Bak*, 1996; *Jensen*, 1998].

[7] Conclusions, thus far for snow and sandpile avalanches are that they do not strictly obey all the criteria for SOC but some of the characteristics of SOC are followed. These conclusions are based mainly on analysis for the first two criteria for SOC listed above. This paper contains analysis relevant to the third part of SOC: the time arrival of avalanche masses. The conclusions are drawn from slab avalanches recorded over twenty consecutive winters (1981–2001) for two avalanche areas for about ten thousand avalanches. The records provide time series with lengths of more than 8,000 time intervals which can be used to study the time-frequency signature aspect suggested for SOC. The results, together with those of *McClung* [2003a], again show that some characteristics of SOC originally defined by *Bak et al.* [1987] are satisfied but if the criteria outlined by *Bak et al.* [1987] are strictly applied then SOC is not satisfied for slab avalanches. The combined results are demonstrated for a physical phenomenon (slab avalanches) from field measurements, estimates, and observations without resorting to computer modeling so that they may contribute to the physical constraints needed to refine the definition of SOC to make it applicable to natural phenomena in a meaningful way.

[8] If SOC does not apply to natural avalanche events (snow and sandpile avalanches) then there is need for information to illustrate the characteristics of these natural, unstable systems. The analysis in this paper is intended to contribute to the information base. Slab avalanches, similar to earthquakes, are destructive, catastrophic events which initiate by fracture propagation. The information in this paper may help to link natural events within a system definition.

2. Character of Time Series Data

[9] The data consist of avalanche events recorded by professional avalanche forecasters for two avalanche areas in British Columbia. Kootenay Pass is located in southeastern British Columbia along a stretch of highway with approximately 50 large avalanche paths affecting the highway and Bear Pass is a stretch of highway in northwestern British Columbia with also about 50 large avalanche paths affecting the highway. Typically approximately 200 days, 1 November through May, constitute the avalanche season each year during which avalanche events are recorded each day by the forecasters. The data included were collected daily for 20 winters from 1980–1981 through 2000–2001.

[10] The snow climates and terrain features may differ for Bear Pass and Kootenay Pass and geographically they are separated from each other by a distance of 1000 km in a northwest southeast line. Bear Pass has numerous very large avalanche paths with start zones in high alpine terrain with few influences of vegetation or forest cover. Kootenay Pass has much smaller start zones and avalanche paths on average than Bear Pass. *McClung and Tweedy* [1994] found the variables which are significant predictors of avalanche activity at Kootenay Pass and *Floyer and McClung* [2003] did the same for Bear Pass. In spite of the geographical separation, the predictor variables are very similar. Mean annual snowfall is about 12 m for Kootenay Pass and it is about 15 m for Bear Pass but the avalanche season typically lasts longer at Bear Pass. These data suggest that since avalanche frequency is related to snow supply, a comparable frequency of avalanching is expected for both areas. However, terrain features suggest larger accumulated masses from storms at Bear Pass due to larger avalanche paths there.

[11] The avalanche occurrence data were recorded on the five-part Canadian size classification scale [e.g., *McClung and Schaerer*, 1993, p. 253]. The classification scale is based on destructive potential and it includes an important order of magnitude estimate of the avalanche mass with mass increasing by about an order of magnitude for each step in size: size 1 is about 10 t, size 2 is about 100 t, size 5 is about 100,000 t. There are other attributes to the size system such as path length scale. However, the most important variable is the avalanche mass. Accordingly, it is assumed for this study that sizes recorded are converted into mass according to: $\text{mass} = 10^{\text{size}}$ with the mass expressed in metric tons. The data were often recorded using half sizes and the same conversion formula was used. For example, size 2.5 was assigned a mass of 316 t. This method of mass conversion is an approximation but for order-of-magnitude estimates required here it should have sufficient accuracy.

3. Time Series

[12] Avalanche events and snow and weather data are collected for avalanche forecasting purposes at Kootenay and Bear Passes. For numerical avalanche forecasting, avalanche events must be roughly correlated with the snow and weather observations. *McClung and Tweedy* [1994] successfully developed a computer assisted avalanche forecasting model for Kootenay Pass. For the model, recorded avalanche events were placed in two daily time periods of roughly 12 hours. This same time frame for data records was used to construct the time series in this study. Thus avalanche occurrence events were lumped into two time periods per day: those recorded before 1200 LT, and those recorded after 1200 LT until approximately 0000 LT.

[13] The time series were constructed by adding all the masses of avalanches recorded during each of two time periods per day by the mass conversion formula given above to give order-of-magnitude estimates of mass for approximately 50 avalanche paths for each time period. Of course, there are many time periods with no avalanches recorded and these records were given $\text{mass} = \text{zero}$ and $\ln(\text{mass}) = 0$. The time series were constructed by placing

the data records for each winter sequentially with summer periods excluded. Therefore the constructions do not represent true time series since summer and fall periods were excluded. Had summer and fall periods been included, no additional useful information about time arrival of avalanche events would result. Further, had summer and fall time periods been included, the generating perturbation for producing avalanches (snow storms) would have been switched off over half the year and the stationary assumption (discussed below) would not be viable. However, the data include all periods when avalanches are possible by application of perturbations from weather conditions and by human influences e.g., avalanche control. Since the focus of this paper is on an examination of time arrival of avalanche events it seems reasonable to exclude the time periods in summer and fall when avalanches are not possible. Taken together, the time series consist of more than 8000 sequential total avalanche mass arrival records for each of Bear Pass and Kootenay Pass. The series contain avalanche mass arrival records consisting of more than 5000 of avalanches for each avalanche area.

[14] Size one avalanches are mainly loose snow avalanches (sluffs) in the Canadian size system. Some size 1 avalanches are present in the databases but only to a limited extent. For the mass sums represented by the databases, the effects of loose snow avalanches will be small or negligible. Thus it can be taken that the time series used in this paper largely represent the mass arrival signature of slab avalanches. Size 1 avalanches are often not recorded by avalanche forecasters since they often stop high above the highways with no effect on operations. Also, observations of them are often obscured by poor visibility associated with storms and mountain weather.

[15] The study of McClung [2003a] was targeted toward size scaling as related to spatial self-similarity for snow slab avalanches and the time series for mass arrival in the present study also apply to slab avalanches. McClung [2003a] and Bažant *et al.* [2003] showed that for individual slab avalanches there is an important length scale which governs the size: the slab depth D to the weak layer. Since the depth to the weak layer can only vary considerably if studied over significantly large areas over a long time, SOC for the snow slab is only possible if the “system” studied applies to large spatial areas over long times. Therefore, if SOC is to be applied, it must be studied in the context of an ensemble “time and spatial average” over a significant area with thousands of events allowing variations in D over several orders of magnitude. Thus the present study is oriented toward that concept with avalanche events summed twice daily for each of the two avalanche areas to study the time arrival aspect of SOC.

3.1. Avalanche Triggers

[16] The time series used in this study consist mostly of slab avalanches which occurred either naturally (without human intervention) and by application of explosive control. In the analysis below, the time series were analyzed according to natural and human triggered events. For Bear Pass, the analysis below includes just the natural events but analysis of all the events together showed that the conclusions are not altered. For Kootenay Pass, similar conclusions follow except that at Kootenay Pass recent years have been char-

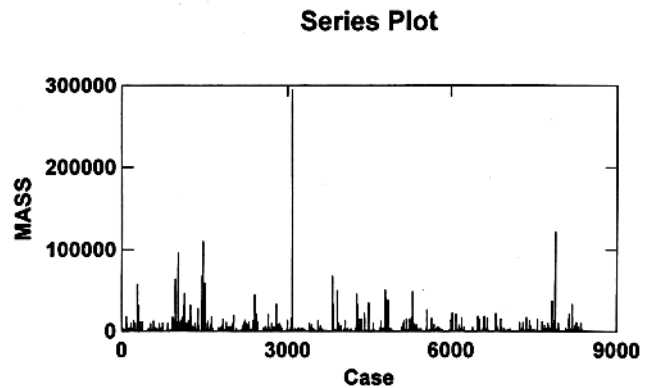


Figure 1. Mass arrival versus time at Bear Pass: 1980–1981 through 2000–2001. The mass is calculated as the sum of masses during two 12 hour periods per day for all the avalanche paths at Bear Pass. Only natural events are included.

acterized by more extensive application of explosives such that the “time flow of events” may have been altered to affect the stationary assumption for the series.

3.2. Stationary Assumption

[17] Physically, a stationary process implies that the random mechanism which generates the process does not change as time progresses. In this paper, the generating process consists of snow storms and weather conditions which produce snow instability in the regions. Climate change could alter this generating process but there are no data to suggest that such is the case for the data analyzed in this paper. Individual avalanche events clearly do not qualify as a stationary process because they involve a single event over a short time interval. In order to qualify as a stationary process, a shift in the time axis describing the flow of events should not alter the conclusions. The remark above about more vigorous application of avalanche control to release avalanches at Kootenay Pass in the past 10 years makes the stationary assumption more questionable than for Bear Pass for which the data consist only of natural events. This problem could be dealt with for Kootenay Pass by splitting the series into two 10 year time series but this is not necessary for the arguments in this paper and it is beyond the scope here.

3.3. Presentation of Time Series and Assumptions

[18] Figure 1 shows the time series of natural avalanche events for Bear Pass. The data from the years 1980–1981 through 2000–2001 are represented. In Figure 1, the avalanche events are “naturals” without application of explosives so the assumption of stationarity should be fulfilled: the same process controls the flow of events throughout the duration of the series.

[19] Figures 2 and 3 show similar time records for Kootenay Pass. Figure 2 shows all avalanches (natural and explosive controlled), and Figure 3 shows just the natural events at Kootenay Pass. Comparison of these figures suggests that for Kootenay Pass the assumption of stationarity is not as good as expected for Bear Pass.

[20] For the analysis in this paper, the data from Figure 1 (Bear Pass naturals) has been used for most of the analysis since it is expected that the stationary assumption will be a

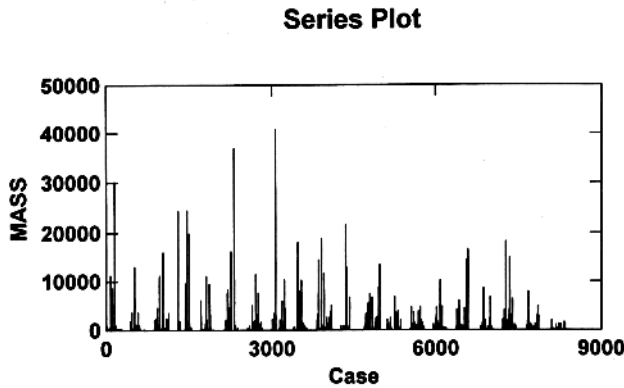


Figure 2. Mass arrival versus time at Kootenay Pass: 1980–1981 through 2000–2001. The mass is calculated as the sum of masses during two 12 hour periods per day for all the avalanche paths at Kootenay Pass. All events, natural and explosive controlled, are included.

good one. Conclusions will also be drawn from Kootenay Pass (Figure 2, all avalanches) but the stationary assumption is probably not as good for the entire series.

[21] From inspection of Figures 1–3, it is suggested that the time series may display some of the aspects of time arrival signature for $1/f^\beta$ noise: the time series do not represent white noise. In the time series (e.g., Figures 1 and 2) there is correlation between from one value to the next and but there are large peaks and fluctuations in the series. Nor are the series periodic with a single fixed frequency or even a few fixed embedded frequencies. This was proven by calculating periodograms for Bear Pass and Kootenay Pass which showed many frequencies contribute to the spectrum. Autocorrelation functions were used to make inferences about the power spectra in this paper as shown below. Since the power spectrum is the Fourier transform of the autocorrelation function, knowledge of the autocorrelation function is mathematically equivalent to knowledge of the power spectrum [Box and Jenkins, 1976].

[22] Inspection of the time series in Figures 1 and 2 reveals that they are strong candidates for at least some characteristics of what Bak et al. [1987, 1988] describe as $1/f^\beta$ noise. However, it is not obvious, meaning that when transformed into the frequency domain, the power spectrum falls off with a negative power of the frequency and most of the power is in the low-frequency (high-magnitude) events. Further analysis is given below.

4. Probability Density Function for Mass Magnitudes

[23] Figures 4, 5, and 6 are probability plots for summed mass magnitudes corresponding to Figures 1 (naturals, Bear Pass), 2 (all avalanches, Kootenay Pass), and 3 (naturals, Kootenay Pass). Figures 4, 5, and 6 imply that the pdfs of mass (t) summed in time intervals obey a lognormal distribution or equivalently, $\ln(\text{mass})$ obeys a Gaussian distribution. In spite of a comparable time length for both series (20 winters) and comparable number of avalanche paths, the mean of $\ln(\text{mass})$ is larger for Bear Pass (mean = 6.67, SD = 1.76, $N = 1940$ cases) than for Kootenay Pass, all avalanches

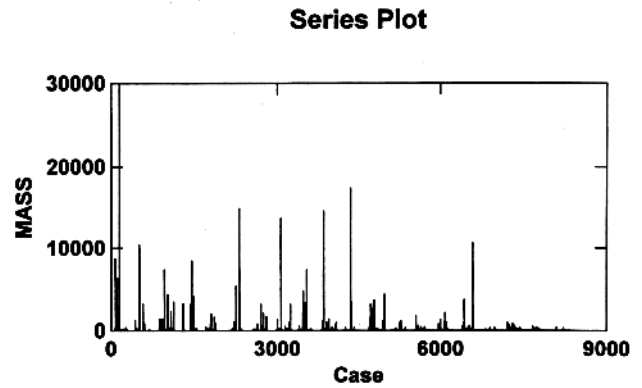


Figure 3. Similar to Figure 2 but including only natural events.

(mean = 5.95, SD = 1.69, $N = 1133$ cases) and I suggest that this is due to the higher number of very large avalanche paths at Bear Pass compared to Kootenay Pass. McClung [2003b] presented a study of magnitude and frequency of avalanches from Bear Pass and Kootenay Pass which illustrates the differences in terrain and avalanche magnitude for the two areas.

[24] Notice that for small mass sums at both Bear Pass and Kootenay Pass, there is a lack of fit on the probability plots. This is due to single small avalanches which are mostly loose snow avalanches of size 1 (the lower limit of the size system). Also, for Kootenay Pass there is a lack of fit at the highest masses for Figure 5. Figure 6 includes just the natural avalanches and the lack of fit at high mass sum does not occur. Therefore it is suggested that for natural avalanches the lognormal pdf is followed for both areas and

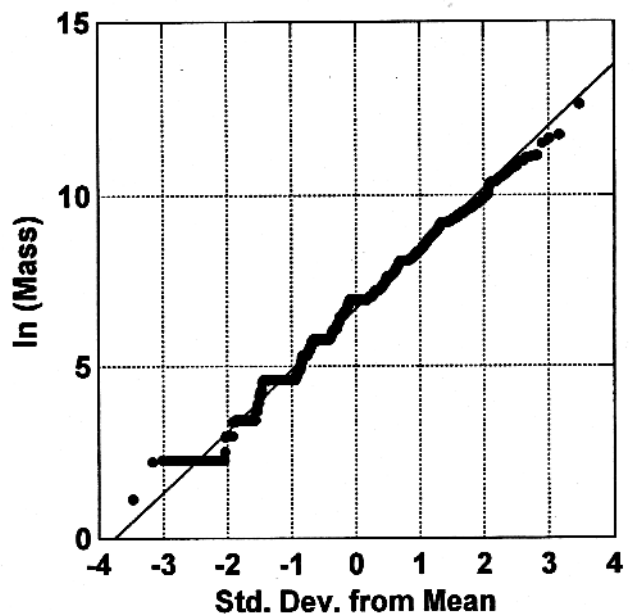


Figure 4. Probability plot for summed arrival masses for the data in Figure 1 from Bear Pass. It is suggested that $\ln(\text{mass summed})$ follows a Gaussian distribution which is represented by the least squares line.

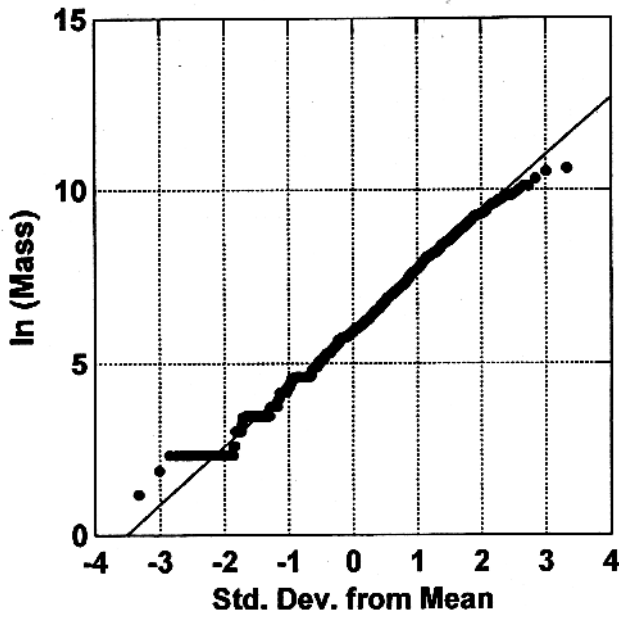


Figure 5. Probability plot for summed arrival masses for the data in Figure 2 from Kootenay Pass (all avalanches). Similar to Figure 4 suggesting that $\ln(\text{mass summed})$ follows a Gaussian distribution.

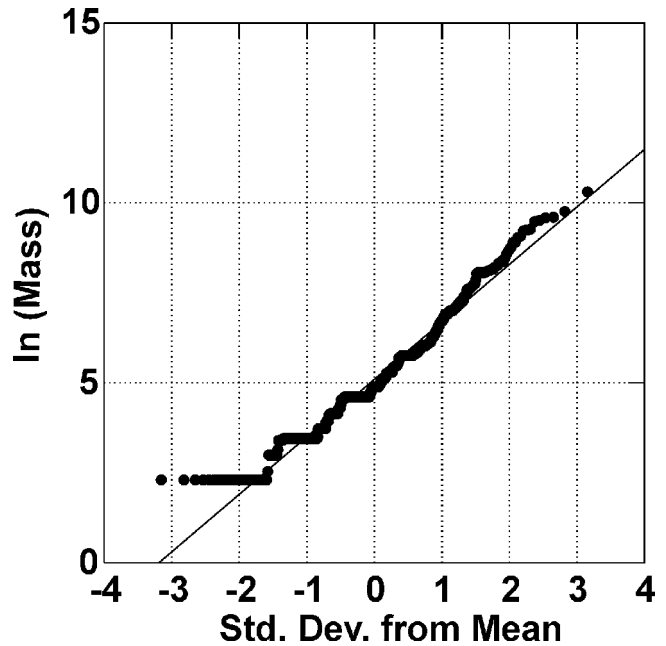


Figure 6. Probability plot for summed arrival masses for the data in Figure 3 (natural avalanches) from Kootenay Pass. It is suggested that $\ln(\text{mass summed})$ follows a Gaussian distribution. In comparison to Figure 5, the lack of fit at high masses is less evident which suggests that the effects of avalanche control may be present in Figure 5.

the lack of fit at high mass for Kootenay Pass is due to application of avalanche control: the actual masses appear to be less than if they had come naturally. The primary goal of application of avalanche control is to reduce the expected avalanche sizes so this effect is not surprising.

5. Autocorrelation Plots for Bear Pass and Kootenay Pass

[25] In order to assess the characteristics of the time series in the frequency domain, it is useful to construct autocorrelation plots. Given an autocorrelation function then the power spectrum in the frequency domain is obtained by its Fourier transform. For $1/f^\beta$ noise as described by *Bak et al.* [1987, 1988] and *Jensen* [1998] it is required that points in the time series are correlated to previous times and that the power spectrum is not constant. The power spectrum should fall off as frequency increases with most power contained in the low-frequency portion of the spectrum.

[26] Figures 7 and 8 show the first-order autocorrelation functions ($\ln(\text{mass})$ with means removed) for Bear Pass (naturals) and Kootenay Pass (all avalanches). Before calculating the autocorrelation functions, smoothing was applied to the series by a moving average over 2 lags. This was done to smooth the data to allow for the possibility of uneven recording between the two 12 hour periods for each day which the data were stratified into. A moving average filter with weights: 1:2:1, respectively, was also applied and the results were not significantly altered. Such 1:2:1 smoothing is known to have little effect on the frequency implied by the spectrum. Figures 7 and 8 show that the autocorrelation functions (ACF) fall with an exponential-like dependence in a rapid manner. According to *Box and Jenkins* [1976] such rapid decline suggests the series may be

stationary. Further, *Box and Jenkins* [1976] show that time series associated with such behavior do not represent white noise. Instead, it is implied that the power spectra (the Fourier transform of the autocorrelation functions) fall off rapidly with frequency with most "power" in the low-frequency portion. Figures 7 and 8, then, suggest that the time series satisfy some of the basic the conditions for $1/f^\beta$ noise. Figures 7 and 8 include significance testing. If the autocorrelation function falls within the solid lines included

Autocorrelation Plot

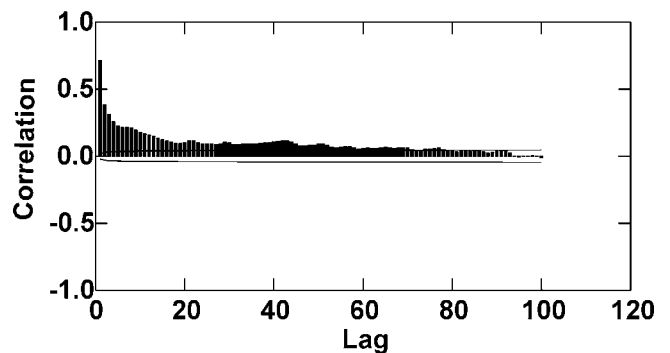


Figure 7. First-order autocorrelation function for the time series in Figure 1 from Bear Pass. The autocorrelation function is calculated for $\ln(\text{mass})$ with the mean removed from the series. The horizontal lines represent the limits of two standard errors (or 95% confidence limits): correlations inside these lines are not significant. The data were smoothed using a moving average of two lags.

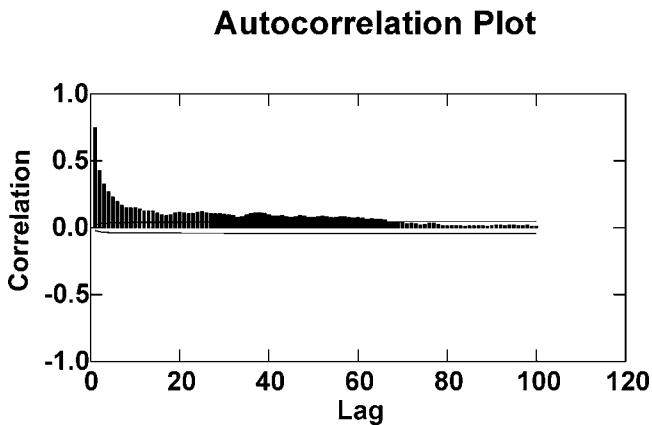


Figure 8. Similar to Figure 6 for the time series in Figure 2 from Kootenay Pass. The horizontal lines represent the limits of two standard errors (or 95% confidence limits): correlations inside these lines are not significant. The data were smoothed using a moving average of two lags.

on the plots, correlations are not significant. The solid lines represent 95% confidence limits for the significance of the correlations.

[27] Figures 7 and 8 are represent autocorrelations of the series $\ln(\text{mass})$ with only the mean removed and minimal smoothing (2 lag moving average). The calculations suggest a rapid decline indicating autocorrelations drop rapidly in a few lags. It is implied that the series from Bear Pass and Kootenay Pass have correlations which drop to about $1/e$ of their initial values of one in a few lags. This suggests the power spectrum declines rapidly, as expected for the $1/f^3$ noise [e.g., Bak, 1996]. The autocorrelation functions also show that the values in the series are correlated with previous values which Bak [1996] explains is a necessary feature of SOC. The timescale for dropping to $1/e$ for both series corresponds approximately to one standard deviation of avalanche arrival time of about 1 day during and after storms. This is shown below with simple modeling concepts.

[28] The autocorrelation functions in Figures 7 and 8 are very nearly identical and they fall off with an exponential dependence. Empirically, both ACFs decline exponentially to a value of about 0.1 at lag 20 with very slow decline after lag 20. I fitted the ACFs over the first 20 lags with a nonlinear numerical model of the form: $0.1 + C1 \exp(-u/C2)$, where u is lag, $C1$ and $C2$ are constants. For Kootenay Pass, I obtained: $C1 = 0.91$, $C2 = 2.3$ with 95% confidence limits on $C2$ between 2.1 and 2.6 ($R^2 = 0.99$, where R is the Pearson correlation coefficient). For Bear Pass, the results were: $C1 = 0.88$, $C2 = 2.4$ with 95% confidence limits between 2.1 and 2.6 ($R^2 = 0.97$). These results suggest that empirically the ACF has an initial exponential decline with an e -folding time of about 2 lags (or 1 day). I also fitted the ACFs over the first 20 lags with a similar function containing $\exp -u^2$ but the fit was not nearly as good as with the function $\exp -u$.

6. Partial Autocorrelation Functions

[29] Theoretically [Box and Jenkins, 1976], the autocorrelation function extends to infinity. Partial autocorrelation

function (PACF) plots show the relationships of the values in the series after partialing out the influence of the intervening points. The PACF plots reveal effects which do not depend linearly on the previous autocorrelations. Figures 9 and 10 show the PACF plots for Bear Pass (naturals) and Kootenay Pass (all avalanches) calculated after removing the mean and smoothed with moving averages of two lags as for the ACF plots. The correlations are significant to about 20 lags. Box and Jenkins [1976] present techniques to classify time series on the basis of ACF and PACF plots. According to Box and Jenkins [1976] when both the ACF and PACF decline rapidly in an exponential manner, such as the examples here, it suggests that the series are mixed processes combining autoregressive and moving average components. It is beyond the scope of the present paper to develop forecasting models from the series here. In a later section, I develop a model for estimating the return period for summed avalanche masses which may be used in planning. For SOC, the most important results are that the ACF and PACF plots fall off exponentially and the form of the power spectrum is suggested by the Fourier transform of the ACF plot.

7. Power Spectrum for Poisson Process as Shot Noise

[30] The previous results show that the autocorrelation functions for the series display exponential decay. Autocorrelation functions of time series are rather analogous to histograms for analyzing the statistical frequency of occurrence of a variable [Box and Jenkins, 1976]. Since the autocorrelation functions are calculated directly from the time series, inferences made from them are probably the best information available for making conclusions. However, they do not provide direct information about the power spectrum. In this section, information derived from the autocorrelation functions is combined with a simple physical model in an attempt to illustrate some possible features of the

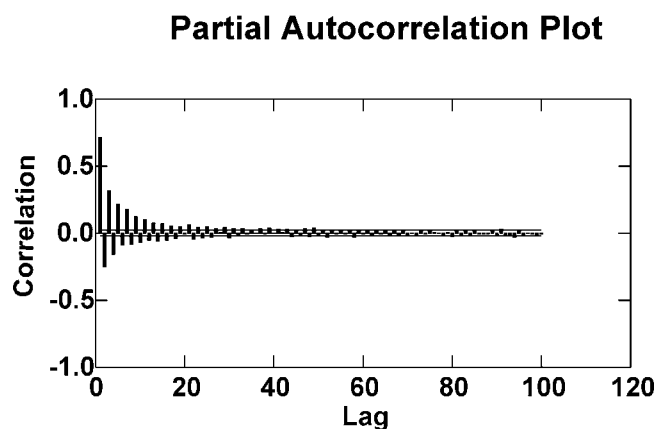


Figure 9. Partial autocorrelation function for the time series in Figure 1 from Bear Pass. The partial autocorrelations are calculated for $\ln(\text{mass})$ with the mean removed from the series. The horizontal lines represent the limits of two standard errors (or 95% confidence limits): correlations inside these lines are not significant. The data were smoothed using a moving average of two lags.

Partial Autocorrelation Plot

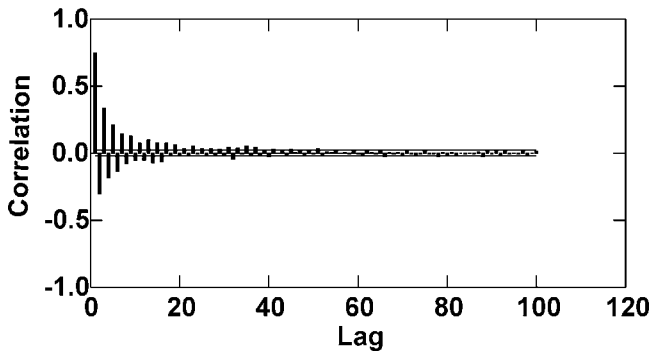


Figure 10. Similar to Figure 8 for the time series in Figure 2 from Kootenay Pass. The horizontal lines represent the limits of two standard errors (or 95% confidence limits): correlations inside these lines are not significant. The data were smoothed using a moving average of two lags.

implied power spectra. However, the conclusions drawn depend on model assumptions so that there is more uncertainty about conclusions which arise from the analysis than from the autocorrelation functions. Given this limitation, I now employ a simple model which is consistent with the autocorrelations and some of the known facts about avalanche events.

[31] Avalanches events are rare, discrete independent events for which arrival may be characterized approximately by a Poisson process under an applied loading perturbation [McClung, 1999]. This approximation holds provided enough time is considered between events to form new weak layers and for new or drifting snow to fill in old fracture lines. Also, avalanche events at one location (e.g., in an avalanche path) are independent of events in another location (e.g., an adjacent avalanche path). In this section, I model avalanche arrivals as a compound stationary Poisson process by superposition of random avalanche events arriving at random Poisson times. The modeling is applied to time series for the avalanche areas by assuming that each avalanche path is characterized by Poisson events which are independent of each other and events in other paths. The modeling is then applied to the entire avalanche area consisting of an ensemble of avalanche paths. The following assumptions apply:

[32] 1. The number of arrivals $N(t)$ for time $t > 0$ is a Poisson process with an average arrival rate ν .

[33] 2. The amplitudes of the summed mass arrivals are characterized by Y_i given by: $\ln(\text{mass})_i$ (summed in a time interval) represented as a Gaussian probability density function (pdf) with zero mean (the mean is removed from the series) and variance σ^2 . This assumption comes from the analysis of the series for Bear Pass and Kootenay Pass (Figures 6 and 7). The ACF plots were derived from these with the means removed.

[34] 3. The arrival times of summed masses at the avalanche areas are Poisson arrival times, τ_i .

[35] 4. The impulse response function representing the distribution of arrival times, $f(t - \tau) = 0$ for $(t - \tau) < 0$ and the function decays such that $f(t - \tau) \rightarrow 0$ for $(t - \tau) \rightarrow \infty$. Thus the random train of summed mass events is such that

one can consider the autocorrelation function to be derived from times which range to infinity corresponding to a stationary process since the autocorrelation functions of the series suggest an exponential or rapid decay.

[36] 5. It is assumed that the arrival times of summed avalanche masses, τ_i and the values of the $Y_i = \ln(\text{mass})_i$ (summed avalanche masses in a time interval) are mutually independent. This is clearly an approximation but since individual avalanche events are independent of others nearby, it is implied that summed masses are derived from mutually independent events. The arrival of naturally triggered avalanche masses depends on snow, weather and storm conditions coupled with the presence of weak layers in the snowpack. Some storms produce no avalanches, other storms produce many with a random number of avalanches with sizes that can vary. Large avalanches can occur singly or many together. Small storm loads can produce large avalanches and large storm loads can produce small avalanches. Birkeland and Landry [2002] emphasized these characteristics for system (avalanche area) response to storm loading. The time series plots for Bear Pass and Kootenay Pass show a fairly random time occurrence for summed avalanche mass arrivals and I suggest this is coupled to random arrival of storms in combination with the presence of weak layers within new storm snow and older weak layers present before storm arrival.

[37] The independence assumption simplifies the analysis, but it is expected to be a reasonable in some instances. For large avalanches to occur, a deep weak layer is needed and this is often independent of the snow and weather conditions which provide the trigger. For the large avalanche cycles in the February 1999 in the Alps, the weak layer they failed on was produced early in the winter more than a month before the arrival of the large storms which produced the avalanches. This situation is common: deep weak layers which are responsible for large avalanches and big avalanche cycles are often formed by snow and weather conditions which preceded the storm triggering events by weeks or months: the trigger and the weak layer on which failures take place can be essentially time independent [Haegeli and McClung, 2003]. Such events at locations in an avalanche area are rare, discrete, independent events with time arrival governed by the perturbation applied by storm loading.

[38] Given the assumptions above, let $X(t)$ be a random, stationary process given by

$$X(t) = \sum_{i=0}^{\infty} Y_i f(t - \tau_i), \quad (1)$$

where the amplitudes Y_i are $\ln(\text{mass})_i$, derived from summed avalanche mass arrivals in an avalanche area with zero mean and variance σ^2 . The arrival times, τ_i , are random, Poisson arrival times, with mean value ν , taken initially to be exponentially distributed with a pdf given by a shifted exponential function:

$$\begin{aligned} f(t - \tau_i) &= f(\theta) = (1/\tau_0) \exp(-\theta/\tau_0) & (t - \tau_i) \geq 0 \\ f(t - \tau_i) &= 0 & (t - \tau_i) < 0. \end{aligned} \quad (2)$$

Physically and observationally, arrival times of avalanches following applied perturbation loading (e.g., snowfall) must

decline rapidly since most avalanches occur during and after storms. For the above assumptions, the autocorrelation function at lag u for the random process [e.g., *Sólnes*, 1997, p. 278] is

$$R_X(u) = \nu\sigma^2 \int_{-\infty}^{\infty} f(\theta)f(\theta+u)d\theta. \quad (3)$$

The power spectral density is the Fourier transform of the autocorrelation function on the infinite domain. It is easily calculated as ($\omega = 2\pi f$ where F is the frequency)

$$S_X(\omega) = \frac{1}{2\pi} \int_{-\infty}^{\infty} R_X(u)\exp(-i\omega u)du. \quad (4)$$

For the arrival function, $f(\theta)$, in equation (2), the implied autocorrelation function, R_X , and power spectrum, S_X , are given by

$$R_X(u) = \frac{\nu\sigma^2}{2\tau_0} \exp(-u/\tau_0) \quad (5)$$

$$S_X(\omega) = \frac{\nu\sigma^2}{2\pi} \frac{1}{1 + \omega^2\tau_0^2}. \quad (6)$$

If a half-Gaussian function is used for $f(t - \tau_i)$, it is implied that

$$\begin{aligned} f(t - \tau_i) &= \frac{2}{\tau_0\sqrt{2\pi}} \exp\left[-(t - \tau_i)^2/2\tau_0^2\right] & t - \tau_i \geq 0 \\ f(t - \tau_i) &= 0 & t - \tau_i < 0. \end{aligned} \quad (7)$$

Integration gives

$$R_X(u) = \nu\sigma^2 \frac{\exp[-u^2/4\tau_0^2][1 - \operatorname{erf}(u/2\tau_0)]}{\tau_0\sqrt{\pi}}, \quad (8)$$

where $\operatorname{erf}(x)$ is the error function,

$$\operatorname{erf}(x) = \frac{2}{\sqrt{\pi}} \int_0^x \exp(-t^2)dt.$$

Similarly, the power spectrum is

$$S_X(\omega) = \frac{\nu\sigma^2}{2\pi} \exp(-\omega^2\tau_0^2) \left\{ 1 - \left[\operatorname{erf}\left(i\omega\tau_0/\sqrt{2}\right) \right]^2 \right\}. \quad (9)$$

Equations (5) and (8) display exponential forms approximately comparable to the autocorrelation functions calculated for the time series and the Dirichlet condition is satisfied: the integral of the absolute value of $R_X(u)$ over the infinite domain is finite.

[39] The autocorrelation functions in equations (5) and (8) suggest decay from an initial value at lag 0 (normalized to one) to $1/e$ of the initial value at lag zero (e -folding time) or approximately $u \approx 1$ to $2\tau_0$. For both Bear Pass and Kootenay Pass (Figures 7 and 8), the autocorrelation func-

tions drop to $1/e$ from their initial values of one at lag 0 on a timescale of about 2 lags. From equations (5) and (8), an approximate value for τ_0 is suggested to be about 1 day which is a reasonable number for the standard deviation of avalanche arrivals during and after storms. The Nyquist frequency, $f_N = 1/(2\Delta t)$, where Δt is the sampling interval (1/2 day) represents an upper limit frequency for the series which corresponds to a timescale of one day in this case. No information is available for higher frequencies or shorter timescales.

[40] Equation (6) implies that $S_X(f) \sim 1/f^2$ at high frequencies where $F = \omega/2\pi \gg 1/(2\pi\tau_0)$ with τ_0 estimated to be about 1 day by analysis from empirical fits to the autocorrelation functions. This suggests a timescale of less than a day (e.g., several hours) with the spectrum behavior $S_X(f) \sim 1/f^2$ being cut off for lower frequencies. A spectrum form $S_X(f) \sim 1/f^2$ is compatible with one expected for SOC [e.g., *Jensen*, 1998]. However, in this model case, it is suggested that $S_X(f) \sim 1/f^2$ is the high-frequency limit of a Poisson process rather than representation of the spectrum for low frequencies over which significant correlations are implied by the data (as estimated from the autocorrelation functions). From Figures 7–10, the timescale for significant correlations extends to about 10 days (20 lags). In order for the frequency spectrum to comply with SOC as envisioned by *Bak et al.* [1987], the $\sim 1/f^3$ behavior should represent the spectrum at low frequencies, not in a high-frequency limit as this model suggests. Given the data collection methods to construct the series (two 12 hour time periods per day), it is not appropriate to speculate about the form of the spectra for timescales of several hours as would be needed to achieve $S_X(f) \sim 1/f^2$ for this model: such frequencies exceed the Nyquist limit.

[41] Thus, for this model, the power spectrum falls off rapidly as frequency increases and the autocorrelation function displays an exponential dependence similar to those calculated from the actual time series. The model is, of course, strictly a consequence of the assumptions but the behavior is similar to that implied by the actual time series. The autocorrelation functions of the series (Figures 7 and 8) fall off exponentially with finite variance instead of being a spike so it is clearly evident that the time series calculated from the data do not imply white noise. Note that in the limit as $\tau_0 \rightarrow 0$ the autocorrelation function (8) becomes a Dirac delta function and the power spectra (6) and (9) become constant implying white noise which is incompatible with SOC. In equation (1), the impulse function in this case is $f(t - \tau_i) = \delta(t - \tau_i)$ which is equivalent to Dirac delta functions with zero variance for arrival times. This is physically impossible for real event arrivals triggered during and after storms which can last for days.

[42] The spectra in equations (6) and (9) are also compatible with white noise in the limit of very low frequencies [$f \ll 1/(2\pi\tau_0)$] with a suggested timescale of at least several months. Data relating avalanche occurrences to the persistence of weak layers [*Haegeli and McClung*, 2003] show that in rare instances, such persistent weak layers can be responsible for avalanche events with intervals of several months between. Therefore avalanche occurrence data provide partial support for the model here: correlations between events spaced more than several months apart should be

very low with highest correlations found for a timescale (τ_0) of about 1 day.

[43] The spectra in equations (6) and (9) illustrate how the form of the autocorrelation function influences the power spectrum. The autocorrelation functions in Figures 7 and 8 are analogous to histograms [Box and Jenkins, 1976] with similar lack of precision. Given the uncertainty about model assumptions, it is probably not appropriate to explore the exact form of the power spectrum implied in great detail.

[44] The form of the autocorrelation functions (Figures 7 and 8) calculated from the time series will strongly depend on the data collection method. For the present analysis, exact arrival times of individual avalanches near the passes are unknown as would be needed to analyze the high-frequency portion of the power spectra. However, experience with avalanche arrivals shows that they occur both during and soon after storms so that a finite standard deviation (or variance) is appropriate with a value comparable to storm duration on the order of a day.

[45] For the simple model here, the power spectrum depends on the average arrival rate of avalanche masses and the variances of $\ln(\text{mass})$ and arrival time. The shape of the spectrum, which is the important determiner for SOC, is determined by the assumed form of $f(t - \tau_i)$ which is unknown. However, the autocorrelation functions calculated for the series (Figures 7 and 8) have exponential-like forms which are more likely to decay as an exponential rather than a Gaussian form as shown by empirical fits to the autocorrelation functions above. The basic conclusions are as follows:

[46] 1. The power spectra do not represent white noise. This is consistent with SOC since a power spectrum which represents white noise is not compatible with SOC [e.g., Bak, 1996].

[47] 2. Most of the power is in the low-frequency part of the spectrum with an implied timescale of about a day. The exact form of the power spectrum or the exact value of β in $1/f^\beta$ cannot be determined without model assumptions which are uncertain with a large influence on the conclusions.

[48] 3. Close inspection shows that the autocorrelation functions for the time series from Bear Pass and Kootenay Pass appear to be a combination of exponential and sinusoidal waves but the numerical calculations (Figures 7 and 8) show that the dominant feature is the exponential dependence so that equation (6) is slightly preferred over equation (9) as the form of the power spectrum.

8. Asymptotic Return Period Model for Bear Pass

[49] A characteristic implied by the analysis above suggests random arrival times of events and random values of summed avalanche mass. A forecasting model for $\ln(\text{mass})$ for the time series probably has limited application. However, return periods for avalanche masses are of interest for snow removal contracts for the avalanche area. From previous results, it is possible to estimate return periods for the magnitude: $\ln(\text{mass})$. It is assumed that $Y = \ln(\text{mass})$ obeys a normal pdf in the domain $(-\infty, \infty)$ and that time arrivals obey a pdf which is statistically independent of the pdf for Y . From (2), the joint pdf for Y , given arrival times τ , is assumed to be

$$f(Y, t - \tau) = g(Y)h(t - \tau), \quad (10)$$

where $h(t - \tau)$ is defined on $0 \leq (t - \tau) \leq 8$. In equation (10), τ and Y are treated as continuous variables. The probability that $Y > Y^*$ is then

$$P(Y > Y^*) = \int_{Y^*}^{\infty} \int_0^{\infty} g(Y)h(t - \tau)dt dY. \quad (11)$$

By integration, equation (10) reduces to

$$P(Y > Y^*) = \int_{Y^*}^{\infty} g(Y)dY. \quad (12)$$

The average number of time periods per year with avalanche masses which exceed Y^* , ν_{Y^*} , given the number of periods per year when avalanches occur, ν_{0+} , is

$$\nu_{Y^*} = \nu_{0+} \int_{Y^*}^{\infty} g(Y)dY. \quad (13)$$

Equation (13) is equivalent to the reciprocal of the return period $T(Y^*)$.

[50] Now $g(Y)$ is standardized. Let $z = [\ln(\text{mass}) - 6.76]/1.76$, where 6.76 is the mean of $\ln(\text{mass})$ and 1.76 is the standard deviation of $\ln(\text{mass})$ for Bear Pass from sample statistics. Given that $Y = \ln(\text{mass})$ is normally distributed,

$$\nu_{z^*} = \frac{\nu_{0+}}{\sqrt{2\pi}} \int_{z^*}^{\infty} \exp(-z^2/2)dz. \quad (14)$$

Asymptotic expansion of the integral yields

$$\nu_{z^*} = \frac{\nu_{0+}}{\sqrt{2\pi}} \exp(-z^{*2}/2) [(1/z^*) - O(1/z^{*3}) + \dots]. \quad (15)$$

From equation (15), an approximate expression for the return period $T(z^*)$ is

$$T(z^*) = \frac{\sqrt{2\pi}}{C_0} z^* \exp(z^{*2}/2), \quad (16)$$

where C_0 is a constant.

[51] The form of equation (16) was used in a nonlinear numerical model with $T(z^*)$ calculated from Hazen plotting positions and assuming that 97 time periods per year had avalanche occurrences in them based on 1940 avalanche periods in 8388 time records over 20 winters. The numerical result gave

$$T(z^*) = 0.043 z^* \exp(z^{*2}/2), \quad (17)$$

with 95% confidence limits on the constant between 0.043 and 0.044 and standard error given by 0.0003. Equation (17) is calculated for $0.79 \leq z^* \leq 3.36$, $0.050 \leq T \leq 40$ years, $8.07 \leq \ln(\text{mass}) \leq 12.6$. Figure 11 shows the nonlinear asymptotic curve versus the values of T derived from the data points. For the curve, $R^2 = 0.98$. The analysis implies that for about 60% of the time periods when there are

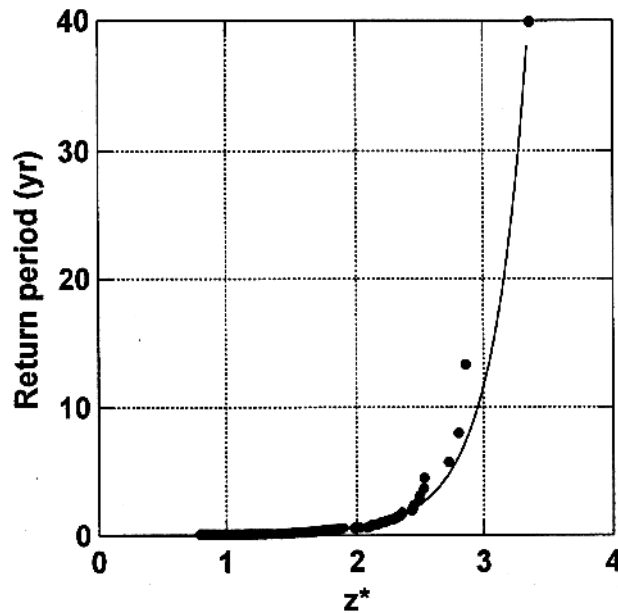


Figure 11. Return period model for summed mass for Bear Pass from the time series in Figure 1. The standardized parameter $z^* = [\ln(\text{mass}) - 6.67]/1.76$, where 6.67 and 1.76 are the mean and standard deviation of $\ln(\text{mass})$.

avalanches, the mass exceeds 3000 t, which corresponds to about three size 3 avalanches. The model and return period calculations suggest that the largest total mass recorded (300,000 t) has a return period of about 40 years at Bear Pass. The return period model has practical implications for estimating snow removal amounts from large avalanche cycles for the highway through Bear Pass.

9. Conclusions and Discussion

[52] On the basis of time arrival of avalanche masses at avalanche areas near Bear Pass and Kootenay Pass, British Columbia, it is expected that the power spectrum in the frequency domain implies rapid decay with frequency and most of the power in the low-frequency part of the spectrum. This behavior is consistent with the frequency behavior for self-organized criticality as postulated by *Bak et al.* [1987, 1988]. The theoretical modeling in this paper contains the assumption that avalanche magnitudes, Y , are statistically independent of arrival times, $(t - \tau)$. However, the conclusions about the power spectra in this paper are independent of this assumption since the conclusions are mostly derived from the form of the autocorrelation functions calculated directly from the series. The theoretical modeling only serves to illustrate some possible forms of the power spectra. Since the exact form of the power spectra cannot be determined without uncertain assumptions, it cannot be stated with certainty that the $1/f^\beta$ spectrum envisioned by *Bak et al.* is implied by the data here.

[53] The frequency power spectra implied by the data analyzed in this paper, when combined with the attempts to analyze spatial self-similarity by *McClung* [2003a], indicate that none of the conditions of self-organized criticality outlined by *Bak et al.* [1987, 1988] can be said

to be completely fulfilled for slab avalanches. All the results of this paper and *McClung* [2003a] are derived from field measurements and analysis about slab avalanches as opposed to computer models. It is believed the two papers represent the first time all three conditions for self-organized criticality have been examined for a critical phenomenon related to mountain slope hazards without resort to computer models. Computer models of natural phenomena may suggest SOC but they do not constitute proof.

[54] The time series in this paper have been derived from time arrival measurements over 20 years representing approximately 10,000 avalanches. This would be difficult or impossible at present for other slope phenomena such as landslides or debris slides due to their low frequency compared to snow avalanches.

[55] If the concepts of self-organized criticality are to be applied for the snow slab, I suggest that the domain should be over considerable time and space such as an avalanche area (many avalanche paths) analyzed over a number of winters. This is linked to the fundamental length scale (slab thickness D) which limits the distribution of sizes in an avalanche area at a given time. In order to obtain a spectrum of avalanche sizes it is necessary to consider a domain which extends over significant scales of time and space. *Jensen* [1998, p. 7] states "For a critical system, the same perturbation applied at different positions or at the same position at different times can lead to a response of any size." If this definition is to apply to snow avalanches then it is implied that the system must be very large in space and/or the timescale must be long. *Jensen* [1998, p. 7] further states: "For systems exhibiting noncritical behavior, the reaction of the system is described by a characteristic response time and characteristic length scale over which the perturbation is felt spatially". Of these two definitions (critical and noncritical systems), the noncritical definition fits most closely with the results in this paper and those of *McClung* [2003a]. The characteristic length scale is D (slab thickness to the weak layer) for individual events. Further, the frequency power spectrum for either Bear Pass or Kootenay Pass might be roughly characterized by a narrow range of time responses associated with storm loading such that a single response time (e.g., τ_0) can approximately describe the process for an avalanche area. The analysis in this paper does not support the suggestion that a plot of $\ln[S_X(f)]$ with $\ln(f)$ is linear over several decades of frequency as is envisioned by *Bak et al.* [1987] for SOC. However, the uncertain assumptions in the analysis and the data collection methods used here prevent conclusions about the exact form of the spectrum, particularly the high-frequency portion.

[56] For avalanches, the time series show there is fundamental uncertainty about the time arrival of events and their magnitudes. For natural hazards, the classical method of dealing with such problems is to estimate the return period for different magnitudes. The asymptotic return period model for Bear Pass shows the practical aspect of the time arrival analysis. It could be used for planning snow removal on a long-term average basis. Time series forecasting models probably would not be successful given the random nature of avalanche arrival by storm loading interacting with snow-pack weak layers to produce large avalanches.

[57] **Acknowledgments.** The research for this paper was supported by Canadian Mountain Holidays, the Natural Sciences and Engineering Research Council of Canada, and the Vice President, Research, University of British Columbia. Data were provided by Snow Avalanche Section, British Columbia Ministry of Highways. I am grateful for all these sources of support.

References

- Bak, P., *How Nature Works*, 212 pp., Springer-Verlag, New York, 1996.
- Bak, P., C. Tang, and K. Wiesenfeld, Self-organized criticality: An explanation of $1/f$ noise, *Phys. Rev. Lett.*, 59, 381, 1987.
- Bak, P., C. Tang, and K. Wiesenfeld, Self-organized criticality, *Phys. Rev. A*, 38, 364, 1988.
- Bažant, Z. P., G. Zi, and D. McClung, Size effect law and fracture mechanics of the triggering of dry snow slab avalanches, *J. Geophys. Res.*, 108(B2), 2119, doi:10.1029/2002JB001884, 2003.
- Birkeland, K. W., and C. C. Landry, Power laws and snow avalanches, *Geophys. Res. Lett.*, 29(11), 49-1–49-3, 2002.
- Box, G. E. P., and G. M. Jenkins, *Time Series Analysis: Forecasting and Control*, 575 pp., Holden-Day, Boca Raton, Fla., 1976.
- Floyer, J., and D. M. McClung, Numerical avalanche prediction in Bear Pass, British Columbia, Canada, *Cold Reg. Sci. Technol.*, in press, 2003.
- Haegeli, P., and D. M. McClung, Avalanche climate of the Columbia Mountains, British Columbia, Canada, *Cold Reg. Sci. Technol.*, in press, 2003.
- Jensen, H. J., *Self-Organized Criticality*, 153 pp., Cambridge Univ. Press, New York, 1998.
- McClung, D. M., The encounter probability for mountain slope hazards, *Can. Geotech. J.*, 36(6), 1195–1196, 1999.
- McClung, D. M., Size scaling for dry slab avalanche release, *J. Geophys. Res.*, 108, doi:10.1029/2002JB002298, in press, 2003a.
- McClung, D. M., Magnitude and frequency of avalanches in relation to terrain and forest cover, *J. Arct. Antarct. Alpine Res.*, 35(1), 82–90, 2003b.
- McClung, D., and P. Schaerer, *The Avalanche Handbook*, 271 pp., Mountaineers, Seattle, Wash., 1993.
- McClung, D. M., and J. Tweedy, Numerical avalanche prediction, Koote-nay Pass, British Columbia, *J. Glaciol.*, 40(135), 350–358, 1994.
- Sólnes, J., *Stochastic Processes and Random Vibrations*, 432 pp., John Wiley, Hoboken, N. J., 1997.

D. M. McClung, Dept. of Geography, Univ. of British Columbia, 1984 West Mall, Vancouver, British Columbia, Canada V6T 1Z2. (mcclung@geog.ubc.ca)